Cold acclimation recruits human brown fat and increases nonshivering thermogenesis

Anouk A.J.J. van der Lans[1], Joris Hoeks[1], Boudewijn Brans[2], Guy H.E.J. Vijgen[1,3], Mariëlle G.W. Visser[2], Maarten J. Vosselman[1], Jan Hansen[1], Johanna A. Jörgensen[1], Jun Wu[4], Felix M. Mottaghy[2,5], Patrick Schrauwen[1], and Wouter D. van Marken Lichtenbelt[1]

First published July 15, 2013 - More info

Research Article (/tags/51) **Metabolism** (/tags/28)

[–] Abstract

In recent years, it has been shown that humans have active brown adipose tissue (BAT) depots, raising the question of whether activation and recruitment of BAT can be a target to counterbalance the current obesity pandemic. Here, we show that a 10-day cold acclimation protocol in humans increases BAT activity in parallel with an increase in nonshivering thermogenesis (NST). No sex differences in BAT presence and activity were found either before or after cold acclimation. Respiration measurements in permeabilized fibers and isolated mitochondria revealed no significant contribution of skeletal muscle mitochondrial uncoupling to the increased NST. Based on cell-specific markers and on uncoupling protein-1 (characteristic of both BAT and beige/brite cells), this study did not show “browning” of abdominal subcutaneous white adipose tissue upon cold acclimation. The observed physiological acclimation is in line with the subjective changes in temperature sensation; upon cold acclimation, the subjects judged the environment warmer, felt more comfortable in the cold, and reported less shivering. The combined results suggest that a variable indoor environment with frequent cold exposures might be an acceptable and economic manner to increase energy expenditure and may contribute to counteracting the current obesity epidemic.

[–] Introduction

Brown adipose tissue (BAT) is a thermogenic tissue, the main function of which is heat production (nonshivering thermogenesis [NST]) when activated by cold exposure. Nowadays, it is well recognized that BAT is present and active in human adults (1–3). Cold-induced BAT activity in humans has been shown by studies determining glucose

uptake using 2-deoxy-2-[^{18}F]fluoro-D-glucose ([^{18}F]FDG) PET/CT scanning (4–6). It has also been well established that BAT activity is inversely related to BMI and body fat percentage, indicating its potential to counterbalance the current obesity pandemic (1, 4, 6). Several studies in humans indeed show that BAT presence and activity are related to NST (3–5, 7), confirming BAT as a target for increasing energy expenditure.

When unacclimatized animals are placed in a cold environment, they will acutely defend their body temperature by means of shivering thermogenesis (muscle contractions), which increases heat production (energy expenditure). However, upon prolonged cold exposure, shivering will gradually decrease, but energy expenditure remains elevated, indicating increased NST (8). In rodents, the increase in NST can be fully attributed to BAT (9, 10). This metabolic adaptation over time is called adaptive thermogenesis (AT). Interestingly, an older study in humans already showed that prolonged cold exposure (12°C, 8 h/d, 31 days) in healthy men also resulted in a gradual decrease of shivering, while heat production remained elevated (11). At that time, the tissue responsible for the observed increased NST in humans was enigmatic, as it was not clear whether human adults possessed sufficient amounts of active BAT. Nowadays, the presence of BAT in human adults is undisputed, but evidence that cold acclimation increases BAT presence and activity is lacking. Nevertheless, human cold acclimation studies show seasonal variation in NST (12), and interestingly, seasonal variation in cold-activated BAT has been reported in humans as well (6); the latter indicates the plasticity of BAT. We therefore investigated the effect of cold acclimation on both NST and BAT presence and activity. Following the "classical" study of Davis on cold acclimation in humans (11), under slightly less severe conditions, 17 healthy subjects (age, 23 ± 3.2 years; BMI, 21.6 ± 2.2 kg/m^2; and fat percentage, 22.3% ± 8.1%), of which 9 were female and 8 were male (Table 1), were acclimated to cold. For 10 consecutive days, subjects were exposed to an environmental temperature of 15–16°C for 6 hours a day. As main outcome parameters we examined BAT activation by cold-induced glucose uptake using [^{18}F]FDG-PET/CT (Gemini TF PET-CT; Philips) imaging and energy expenditure by indirect calorimetry before and after cold acclimation.

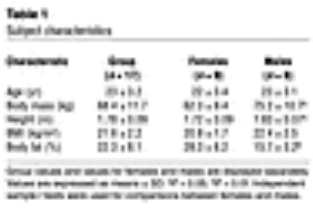

(/articles/view/68993/table/1)**Table 1**

(/articles/view/68993/table/1)

Subject characteristics

[–] Results

Increased NST upon cold acclimation. Before cold acclimation, resting metabolic rate (RMR) was 6.8 ± 1.0 megajoule (MJ) /24 h with females having a significantly lower RMR (6.2 ± 0.7 MJ/24 h) compared with males (7.6 ± 0.7 MJ/24 h) ($P < 0.05$). In order to determine NST, subjects were exposed to mild cold; for this purpose they were wrapped in a water-perfused suit (ThermaWrap Universal 3166 MTRE; Advanced Technologies Ltd.) connected to 2 water heating/cooling systems (Blanketroll III; SubZero). This setup is suitable for use inside the PET/CT scanner. The cooling protocol ensured that subjects were measured during stable nonshivering conditions. This mild cold condition caused a significant increase in energy expenditure, both in females and males (to 6.9 ± 1.0 and 8.5 ± 0.6 MJ/24 h respectively; $P < 0.05$; Table 2). Cold acclimation increased NST significantly from 10.8% ± 7.5% before to 17.8% ± 11.1% after ($P < 0.01$) (Figure 1), but no significant change in RMR occurred ($P > 0.05$) (Table 2). Despite the metabolic adaptation found after cold acclimation, no changes in the time until shivering were observed (50 ± 11 and 51 ± 12 minutes before versus after the cold acclimation period; $P > 0.05$), and similar suit temperatures during the mild cold conditions were used (25.4 ± 1.8 and 25.8 ± 1.6°C before versus after cold acclimation; $P > 0.05$). Therefore, the same mild cold stimulus (absolute suit temperature) resulted in a higher metabolic response after cold acclimation. The absence of changes in shivering threshold might be explained by the relatively short-term and intermittent cold challenge used in this protocol. Another explanation is that body temperature distribution might have changed. No sex differences in NST were observed; NST in females was 11.0% ± 9.8% before and 15.9% ± 10.7% after the cold acclimation, whereas in males an NST of 11.6% ± 4.3% before and 20.3% ± 12.0% after was found ($P > 0.05$).

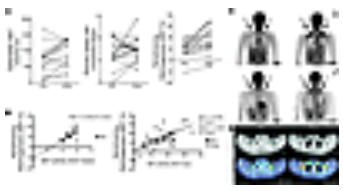

(/articles/view/68993/figure/1)**Figure 1**

(/articles/view/68993/figure/1)

Individual data of BAT activity and NST before and after cold acclimation. Detectable BAT volume and NST increased significantly upon the cold acclimation period. A significant relation is found between NST and BAT activity. (**A**) Individual data on BAT activity. Left panel: detectable BAT volume (cc); middle panel: glucose uptake rate (μmol/min/100 g); right panel: NST (%). Please note that detectable BAT

volume is an overestimation of true active BAT volume. (**B**) Relation between NST and BAT. Left panel: NST expressed as percentage and BAT activity as SUV mean; right panel: NST expressed as percentage and BAT activity as SUV max. (**C**) [^{18}F]FDG-PET images of the upper body after cold exposure in a female (top) and a male subject (bottom), before (pre) and after (post) cold acclimation. Main BAT locations are indicated with black arrows; additionally, paravertebral BAT is activated. (**D**) Transversal CT (top) and PET/CT fusion (bottom) slice of the supraclavicular region demonstrating [^{18}F]FDG-uptake in BAT locations (white arrows) after cold exposure, both before and after the cold acclimation period.

(/articles/view/68993/table/2)**Table 2**

(/articles/view/68993/table/2)

BAT activity and energy expenditure under thermoneutral conditions and during mild cold exposure, before and after cold acclimation

BAT recruitment after cold acclimation. Retrospective studies have suggested a higher prevalence of BAT in females (13); however, the results of the present study do not confirm this. Thus, cold-activated BAT activity before acclimation was 2.3 ± 0.9 mean standard uptake value (SUV mean; uptake kBq/ml/injected dose [kBq]/patient weight [g]), "detectable" (PET-based) BAT volume was 556 ± 448 cc, and glucose uptake rate was 5.4 ± 3.1 μmol/min/100 g in females, whereas male values were not statistically different (2.6 ± 0.3 SUV mean, 788 ± 452 cc, and 8.5 ± 2.0 μmol/min/100 g, $P > 0.05$; Table 2). Since we did not observe sex differences in BAT activity values before cold acclimation, the combined results will be presented below. Before cold acclimation, 94% (16 out of 17) of the subjects showed cold-activated BAT depots, and after cold acclimation, 100% BAT prevalence was observed. Cold acclimation increased upper body BAT activity from 2.4 ± 0.7 to 2.8 ± 0.5 SUV mean ($P < 0.01$) and detectable BAT volume expanded from 665 ± 451 cc before to 913 ± 458 cc ($P < 0.01$) afterwards. Analysis of dynamic PET/CT imaging of the supraclavicular region revealed that upon cold acclimation, glucose uptake rate did not increase significantly (6.9 ± 3.0 vs. 7.6 ± 2.5 μmol/min/100 g; $P > 0.05$). One subject showed a negative NST both before (–10.5%) and after (–5.2%) cold acclimation, which can be due to low or no NST in combination with lower temperatures of the extremities, causing a drop in metabolism in these regions (Arrhenius law) (14). Interestingly, this was

also the subject in which no BAT could be detected before the cold acclimation period and who only showed a small increase of BAT upon cold acclimation. Increase in NST was not related to increase in BAT. However, before cold acclimation, there was a significant positive relation between NST and BAT activity ($r^2 = 0.78$; $P < 0.01$) and NST and maximal BAT activity ($r^2 = 0.55$; $P < 0.01$). After acclimation, NST was still related to maximal BAT activity ($r^2 = 0.32$, $P < 0.05$; Figure 1B). Taken together, these results indicate that human BAT is recruited upon chronic cold stimulation, as in rodents. A significant increase in detectable BAT volume was found, which indicates that more brite or brown adipocytes were activated. The increased maximal glucose uptake (SUV max) in BAT upon cold acclimation indicates an increased metabolic activity of existing BAT. In parallel, NST increased, suggesting involvement of BAT. An individualized cooling protocol was used for the determination of NST and BAT activity; however, the cold acclimation was fixed at 16°C, since this has previously been shown to increase cold-induced energy expenditure (15). No correlation was found between suit temperature and BAT activity and suit temperature and the subjective responses. Moreover, no correlations were found between sensation scores completed during cold acclimation and (the change in) BAT activity. Therefore, we were not able to show a correlation between the magnitude of the cold experience and BAT recruitment.

The role of skeletal muscle respiration in cold-induced thermogenesis. Besides BAT, skeletal muscle (SM) is an alternative putative tissue for NST. Particularly, studies in animals identified mitochondrial uncoupling (proton leak) in SM as a source of heat production in response to cold (16, 17). In humans, it has been shown that SM can be responsible for a 40% increase in total body energy expenditure after epinephrine infusion (18). More recently, we showed in cold-exposed humans that NST is significantly related to estimates of mitochondrial uncoupling in SM, supporting a role for SM in human NST (19). To investigate the role of SM during cold acclimation, we first measured SM respiration in permeabilized muscle fibers using a multisubstrate protocol, similarly to our previous study (19). Samples were taken before and after the cold acclimation period. Cold acclimation did not affect oxygen consumption in any of the respiratory states analyzed. Particularly, state 4 respiration, reflecting mitochondrial proton leak, was similar before and after cold acclimation (125.9 ± 11.2 vs. 138.8 ± 11.8 pmol/(s*mg)/(MtDNA copy numbers) × 10.000, respectively; Figure 2B). In addition, also the maximally coupled (state 3) and maximally uncoupled (state U, reflecting the capacity of the electron transport chain) respiration remained unchanged (Figure 2, C–E), indicating an unchanged SM oxidative capacity.

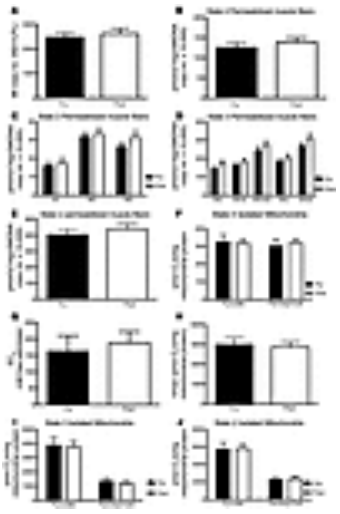

(/articles/view/68993/figure/2)**Figure 2**

(/articles/view/68993/figure/2)

No effect of cold acclimation on SM respiration. (**A**) Mitochondrial density (*n* = 16). Panels **B**–**E** represent the data from permeabilized muscle fibers (*n* = 16, 8 male/8 female) corrected for mitochondrial density, while **G** and **H** (*n* = 11, 5 male/6 female) and **F**–**J** (*n* = 9, 3 male/6 female) reflect the data from isolated mitochondria obtained in a subset of subjects. (**B**) Oxygen consumption not linked to ATP synthesis (state 4). (**C**) Oxygen consumption upon substrates only (malate, malate + octanoylcarnitine, malate + glutamate; state 2). (**D**) ADP-stimulated respiration (state 3) fuelled by various complex I– and complex II–linked substrates. (**E**) Maximally uncoupled respiration upon the chemical uncoupler FCCP. (**F**) Mitochondrial oxygen consumption not linked to ATP synthesis (state 4) on pyruvate and palmitoyl-CoA + carnitine. (**G**) Mean EC_{50} value of palmitate concentration-response curves. (**H**) Mean Vmax of palmitate concentration-response curves. (**I**) ADP-stimulated respiration (state 3). (**J**) Maximally uncoupled respiration upon FCCP fueled by pyruvate or palmitoyol-CoA + carnitine. The effects of cold acclimation on all SM parameters were tested with paired-samples *t* tests. Black and white bars represent the values before and after cold acclimation, respectively. Values are expressed as means with SEM. M, malate; G, glutamate; S, succinate; O, octanoyl-carnitine.

For a more in-depth analysis of mitochondrial uncoupling upon cold acclimation, we also isolated SM mitochondria. In these mitochondria, “basal” mitochondrial oxygen consumption not related to ATP production, i.e., state 4 or leak respiration, was then analyzed on 2 different substrates (i.e., pyruvate and palmitoyl-CoA). In parallel with our findings in the permeabilized muscle fibers, also state 4 respiration fueled by single substrates in isolated mitochondria was unchanged upon cold acclimation (Figure 2F). Since it is well known that fatty acids (FAs) are capable of stimulating mitochondrial respiration that is not coupled to ATP production (i.e., FA-induced uncoupling), possibly due to activation of proteins that facilitate proton leak (20), we next tested the sensitivity of the mitochondria for the uncoupling effects of FAs both before and after cold acclimation. As expected, FAs (palmitate) stimulated leak respiration in SM mitochondria in a dose-

dependent manner (data not shown). Calculated half-maximal effective concentration (EC_{50}) values (163.1 ± 157.1 vs. 188.6 ± 114.6 nM free palmitate) and Vmax values (2999.5 ± 1072.4 before and 2866.1 ± 883.9 pmol O_2/s/mg mitochondrial protein after cold acclimation) were, however, similar, indicating a comparable sensitivity for FA-induced uncoupling before and after the cold acclimation period (Figure 2, G and H). Finally, also maximally coupled (state 3) and maximally uncoupled (state U) respiration remained unchanged upon cold acclimation, both when fueled by either the carbohydrate-derived substrate pyruvate or the FA-derived substrate palmitoyl-CoA (plus carnitine) ($P > 0.05$; Figure 2, I and J).

Taken together, these results do not support the notion that an enhanced SM mitochondrial uncoupling underlies the increased NST upon cold acclimation, which is in line with the 2012 PET tracer study by Ouellet et al., who showed that SM does not contribute to NST (4).

"Browning" of white adipose tissue. Although BAT seems to be the main site for NST in rodents (10), recent findings indicate that within white adipose tissue (WAT), UCP1-positive, "inducible" cells can be found (21). These cells are called *beige* (22) or *brite* (23) adipocytes. Upon activation, these beige/brite cells resemble morphology (many small fat vacuoles and many mitochondria) and function (heat production) of brown adipocytes. Based on cell-specific markers, recent data, also from our group, support a mixed composition of white and beige/brite adipocytes in human depots that were identified as BAT (22). In accordance, Sharp et al. (24) recently confirmed that human BAT can be categorized as beige/brite and not "classical" BAT. In that perspective, recruiting beige/brite cells and transdifferentiation of WAT into beige/brite might be potential targets in body weight regulation. We therefore measured mRNA expression of several BAT, WAT and beige/brite markers in subcutaneous abdominal fat tissue collected before and after the cold acclimation period (real-time RT-PCR primer sequences in Supplemental Table 1 and Supplemental Methods; supplemental material available online with this article; doi: 10.1172/JCI68993DS1 (http://dx.doi.org/10.1172/JCI68993DS1)). None of the measured browning markers were significantly altered in subcutaneous WAT after 10 days of cold acclimation ($P > 0.05$; Supplemental Table 2). These results indicate that cold acclimation did not induce browning of cells within abdominal subcutaneous WAT. A stronger cold stimulation or a longer time period of acclimation might be required for the more general browning of the subcutaneous adipose tissue depot. We also examined gene expression

of the same markers in SM tissue. A significant upregulation in PPARγ (1.03 ± 0.25 before and 1.19 ± 0.34 AU after; $P < 0.05$) and adiponectin was found (1.07 ± 0.71 before and 1.76 ± 1.42 AU after; $P < 0.05$; Supplemental Table 2).

The effects on body temperatures, skin perfusion, blood pressure, and blood values. The individualized cooling protocol used to activate BAT lowered mean skin temperature from 35.2 ± 0.8°C (thermoneutral) to 31.8 ± 1.2°C (mild cold). However, no changes in body temperatures (both skin and core) before and during cold exposure after cold acclimation were detected (Table 3). Hand skin blood flow during cold exposure was reduced to a larger extent after the cold acclimation (–78% ± 17% before, and –88% ± 9% afterwards; $P < 0.05$; Table 3). Systolic blood pressure and mean arterial pressure (MAP) during thermoneutral conditions decreased significantly after cold acclimation (MAP from 82.8 ± 6.8 to 79.5 ± 5.1 mmHg, $P < 0.05$). Before and after cold acclimation, the same values during cold exposure were found due to a stronger increase in MAP (Table 3). All values were within normal ranges of young adult humans (25). Blood values during the thermoneutral condition of insulin, glucose, free FAs, triglycerides, T4, thyroid-stimulating hormone (TSH), CRP, IL-6, and IL-8 did not change after cold acclimation (Table 3). Acute cold increased plasma noradrenaline significantly to the same extent both before and after cold acclimation (from 332.6 ± 123.6 during thermoneutral to 867.5 ± 237.4 ng/l during mild cold conditions before [$P < 0.01$] and from 355.4 ± 127.7 during thermoneutral to 916.7 ± 282.7 ng/l [$P < 0.01$] during mild cold conditions after the cold acclimation period; Table 3), as previously described (26, 27). There were no changes in adrenalin levels upon acute cold stimulation. However, cold acclimation resulted in lower adrenalin levels during thermoneutrality (41.7 ± 17.8 before and 33.7 ± 16.9 ng/l afterwards; $P < 0.05$) and higher levels during mild cold stimulation (34.6 ± 11.8 before and 39.9 ± 18.6 ng/l after cold acclimation; $P < 0.01$).

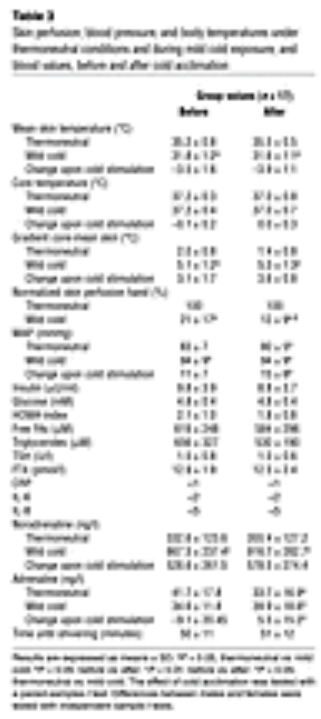

(/articles/view/68993/table/3)**Table 3**

(/articles/view/68993/table/3)

Skin perfusion, blood pressure, and body temperatures under thermoneutral conditions and during mild cold exposure, and blood values, before and after cold acclimation

Changes in subjective responses during cold acclimation. During the cold acclimation period, subjects completed visual analogue scales (VAS scales) (28) on sensation, thermal comfort, and shivering at several time points after entering the cold room (Supplemental Figure 1 and Supplemental Methods). A lower incremental AUC (iAUC) indicates a sensation closer to neutral, lower self-reported shivering, and more comfort. The iAUC decreased with 57% for sensation ($P < 0.05$), 61% for self-reported shivering ($P < 0.01$), and 72% ($P < 0.01$) for comfort. This indicates that, after cold acclimation, the environment is judged as warmer and more comfortable and that self-reported shivering decreased during cold exposure (Figure 3).

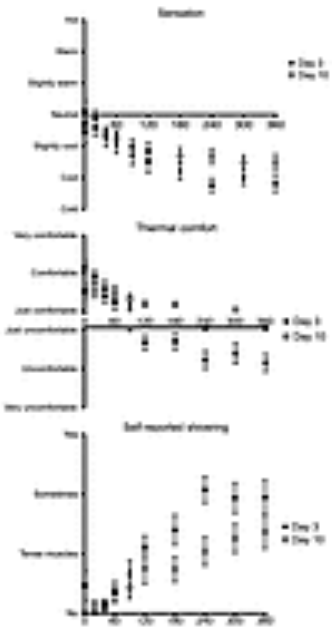

(/articles/view/68993/figure/3)**Figure 3**

(/articles/view/68993/figure/3)

Graphical reflection of VAS scales. A higher sensation and thermal comfort and lower self-reported shivering were reported on day 10 as compared with day 3. The iAUC decreased with 57%, 72%, and 61% for sensation, thermal comfort, and self-reported shivering respectively ($P < 0.05$; $P < 0.01$; $P < 0.01$, respectively). This was tested with a paired-samples *t* test. Values are expressed as means with SEM. Black squares represent the third day of acclimation (first time 6 hours cold exposure); white squares represent the tenth day.

[–] Discussion

There has been revitalized interest in BAT after the discovery of functional BAT in human adults in 2009 (1, 2, 13), not in the least because BAT activation may be able to counteract obesity and type 2 diabetes (27, 29). Although extensive data are available on the plasticity of this tissue in rodents (10, 30), there is an urgent need for studies focusing on BAT recruitment in humans. The current study shows, for what we believe is the first time, highly significant BAT recruitment in human adults after a 10-day period of cold acclimation. Detectable BAT volume increased significantly, by 37%, comparable to the changes occurring in rodents (23, 31). Cold-induced glucose uptake rate expressed in μmol/min/100 g did not increase significantly. However, the combination of both an increased maximal glucose uptake (SUV max) and an increase in detectable volume points toward an increased activity and recruitment of brown adipocytes, as is supported by visual inspections of the PET images (Figure 1, C and D). It should be noted, however, that count spilling caused by the finite resolution of the PET-imaging process is responsible for an overestimation of true active BAT volume both before and after cold acclimation. This study shows that BAT activity and detectable BAT volume, before and after cold acclimation, are similar in females and males. An increase in NST was found after cold acclimation. Moreover, maximal BAT activity was related to NST before and after cold acclimation. Our results are in line with the study by Davis in 1961 (11). The increase in NST upon acute cold exposure in our study was 11% before and 18% after cold acclimation, whereas in the Davis study, using a somewhat longer cold acclimation period with lower temperatures, the average increase in NST after cold acclimation was 34%. The lower NST, both before and after acclimation, in our study may be explained by the use of different cold exposure protocols, as we used individualized mild cold exposure to ensure absence of shivering. These results therefore indicate that human BAT contributes to NST and to the increase of NST during acclimation. These results are in line with an acclimation experiment from our laboratory (32) of even shorter duration (3 days) and under continuous mild cold (16°C). That study revealed a significant increase in total daily energy expenditure (TDEE) without shivering (TDEE increased from 11.5 ± 0.0.1 to 12.1 ± 0.2 MJ/day, corrected for fat-free mass [FFM]). No changes in RMR were found in the current study. The relatively short duration (6 hours/day) in combination with intermittent cold exposure may have been the reason for this. RMR increases are mediated by the thyroid hormone axis. Generally, an increase in thyroid hormone (T3) achieves its effect on RMR after a time span of 7–14 days of continuous cold exposure (33). In this study no changes

in thyroid hormones (TSH, FT4) were found, probably due to the intermittent cold exposure and the short duration of the intervention. No changes in noradrenaline levels were found upon cold acclimation, and adrenaline levels were significantly lower in thermoneutral condition, which is in line with the trend found by Vybíral et al. (34), with winter swimmers having a nonsignificant (trend) lower adrenalin level during cold exposure when compared with control subjects. A possible explanation might be an increased sensibility of the receptor. Cold-induced BAT recruitment may be important in the regulation of body weight and prevention of obesity. However, in the current study, no significant changes in body weight and body composition were observed, which may indicate that increased energy expenditure was compensated by increased food intake or reduced physical activity. Alternatively, for measurable changes in body composition, a longer cold acclimation period may be needed, and future studies with a similar setup, but with an increased duration and with inclusion of dietary instructions, are needed.

Previously we have shown a positive relation between changes in SM mitochondrial uncoupling and the increase in 24-hour energy expenditure after 3 days of mild cold exposure (19, 35). In this study, we could not confirm a relation between changes in NST and SM uncoupling as assessed in permeabilized muscle fibers. Also, a more in-depth analysis of mitochondrial respiration in isolated mitochondria did not reveal changes in mitochondrial uncoupling. Although the type (continuous vs. intermittent) and duration (3 vs. 10 days) of cold exposure may contribute to this discrepancy in results, the present study shows that changes in mitochondrial uncoupling capacity in SM did not relate to the increased NST after cold acclimation in humans.

From cell culture studies, it is now well established that there are 2 distinct types of BAT cells, one derived from myf5-positive lineage (36), called the classical BAT cells, and myf5-negative, called inducible BAT, or beige or brite cells (22, 23). Based on cell-specific markers and on UCP1 (characteristic of both BAT and beige/brite cells), this study did not show browning of abdominal subcutaneous WAT upon cold acclimation. Possible increases in beige/brite cells may have been under the detection level, or browning in deeper depots (visceral, deeper subcutaneous) may have occurred. Unfortunately, we are unable to take WAT biopsies from these areas in our lean, healthy subjects. Furthermore, it remains possible that a longer cold stimulation period may result in a more general browning of human WAT.

MAP during thermoneutrality was reduced after cold acclimation, and a stronger reduction in skin perfusion upon acute cold exposure at the hand was found. The latter may indicate that next to a metabolic response to cold acclimation (increase in NST), also an insulative response has occurred. Together, these physiological adaptations are in line with the change in subjective reporting on cold sensation, as subjects judged the environment warmer, felt more comfortable in the cold, and reported less shivering, indicating that cold was better tolerated. These changes in comfort also indicate that daily mild cold exposure might be a feasible therapy against the obesity pandemic. Earlier studies have shown that temporal exposures to 17°C are acceptable for both adults and the elderly (37). Introducing indoor temperature variations in dwellings and offices may therefore activate BAT and NST and thus impose a healthier indoor environment.

In conclusion, the present study shows that repeated intermittent cold exposures recruited BAT in humans and that this was accompanied by an increase in NST. BAT presence and activity were not different between males and females, both before and after the cold acclimation period. SM mitochondrial uncoupling did not contribute to the increased NST. In addition, the subjective experience of cold shifted to a more comfortable experience. Although more prolonged studies are warranted, a variable indoor environment with frequent cold exposures might be an acceptable and economic manner of increasing energy expenditure and may contribute to counteracting the current obesity epidemic.

[–] Methods

Subjects

All subjects were studied between December 2011 and May 2012. No effect of the cold acclimation on the anthropometric parameters was found (Table 1). All females were on oral contraceptives with the active substances ethinyl estradiol and levonorgestrel and were not measured during their menstruation period to minimize hormonal effects on thermoregulation (38, 39). Exclusion criteria were diabetes mellitus, pregnancy, physical activity more than twice a week, use of beta blockers, and a history of cardiovascular diseases and asthma or other pulmonary obstructive diseases.

Study design

Subjects were exposed to an environmental temperature of 15–16°C for 10 consecutive days: 2 hours on the first day, 4 hours on the second day, and 6 hours per day for the remaining days. Before and after this period the following measurements were performed. In the morning, after an overnight fast, an abdominal subcutaneous fat biopsy (~1 g) was taken, 6–8 cm lateral from the umbilicus under local anesthesia (2% lidocaine) by needle biopsy. Subsequently, a muscle biopsy from musculus vastus lateralis was taken according to the technique of Bergström (40). On a separate day, body composition was determined by means of dual x-ray absorptiometry (type discovery A; Hologic) and was followed by an individualized mild cold experiment. To define BAT activity, [^{18}F]FDG-PET/CT-imaging was used. For this purpose, subjects were measured in the afternoon after a 4-hour fasting period and were asked to refrain from exercise 24 hours before the measurements. A cannula was inserted in the left antecubital vein for blood sampling during thermoneutral and mild cold conditions and injection of the tracer. On 14 ISO-defined (41) sites, iButtons (Maxim Integrated Products) were placed and subjects swallowed a telemetric pill (CoreTemp HT150002; HQ Inc.) for skin and core temperature measurements, respectively. A pressure cuff (Cresta) to measure blood pressure and a chest strap (Polar T31; Polar) for measurement of heart rate were attached. Laser Doppler probes were attached for skin perfusion measurements at the ventral side of the hand at the base of the thumb, at the ventral side of the forearm halfway between the elbow and the wrist (Perimed PF4000; Perimed), at the ventral side of the hallux, and at the abdomen halfway between the umbilicus and the left lateral side of the body (Perimed PF5000; Perimed). Energy expenditure was measured continuously by means of a ventilated hood system (Omnical; Jaeger).

Cold acclimation

During the cold acclimation, subjects performed sedentary activities, such as studying and watching TV, and were instructed to refrain from physical activity. In the cold room, subjects were dressed in shorts and T-shirts. Every 2 hours, a cup with soup or tea was offered, and sandwiches were freely available.

Subjective responses during cold acclimation

On prescribed time points (t = 0, t = 20, t = 40, t = 60, t = 90, t = 120, t = 180, t = 240, t = 300, and t = 360) after entering the cold room, subjects completed VAS scales on sensation, thermal comfort and shivering (Supplemental Figure 1 displays an example of VAS scales completed). The responses of the third day (first time 6-hours cold exposure)

were compared with the responses of the tenth day by means of a paired sample *t* test. The iAUC was calculated to gain more insight in the general effect of the cold acclimation. In total, 13 subjects (7 female/6 male) completed the VAS scales.

Individualized cooling protocol to define BAT presence and activity

Subjects were wrapped in a water-perfused suit, which is suitable for use inside the scanner. The protocol started with a thermoneutral period of 45 minutes, followed by the individualized cooling protocol. Each subject was cooled down (water temperature was lowered by 4°C every 15 minutes) until shivering occurred. After this, subjects were warmed up for 5 minutes so that shivering disappeared, and finally the suit temperature was set slightly above the temperature at which shivering occurred. An estimate of suit temperature was obtained by the average of the inlet and outlet. After 30 minutes of mild cold exposure, the subjects were transported toward the scanner for [^{18}F]FDG-PET/CT imaging.

PET/CT scanning protocol

While subjects were inside the PET/CT scanner, mild cold stimulation continued. Imaging started with a low-dose CT scan (30 mAs, 120 kV), immediately followed by a one-hour dynamic PET scan. At the start of the PET-scanning protocol, subjects were injected with 74 MBq of [^{18}F]FDG intravenously. Images were reconstructed according to the following time frames: 10 × 15 seconds, 5 × 30 seconds, 5 × 60 seconds, 5 × 120 seconds, and 8 × 300 seconds. After the dynamic scan, a static scan as described earlier (1) was performed. The PET image was used to determine the [^{18}F]FDG uptake, and the CT image was used for PET attenuation correction and localization of the [^{18}F]FDG uptake sites. The voxel size of reconstructed PET and CT image sets were 4 × 4 × 4 mm^3 and 1.172 × 1.172 × 4 mm^3, respectively.

PET analysis

The scans were analyzed using PMOD software (version 3.0; PMOD Technologies). Both the researcher (Anouk A.J.J. van der Lans) and an experienced nuclear medicine physician (Boudewijn Brans) interpreted the PET/CT images. We define BAT activity as glucose uptake in fat tissue. The static scan expressed this as SUV mean, with maximal SUV as the maximum value in that region. BAT volume in this study was obtained from PET activity values and called detectable BAT volume. Besides the static scan, we also

performed a dynamic scan to define glucose uptake rate in BAT. The latter was used to construct time activity curves (TACs) of the supraclavicular regions, and the aortic arch was used as an image-derived input function. Glucose uptake rates were calculated using Patlak curve fitting (42) and a lumped constant of 1.14 (43). For the static scan, the regions of interest were manually outlined, and we used a threshold of 1.5 SUV and Hounsfield units between –10 and –180 to define BAT, as described earlier (26).

SM respiration

After the biopsy, a portion of the muscle tissue was directly frozen in melting isopentane and stored at –80°C for determination of mitochondrial DNA (mtDNA) copy number (ratio ND1 to LPL), as described previously (44).

Permeabilization of muscle fibers. A small portion (~30 mg) of the muscle tissue was immediately placed in ice-cold preservation medium (BIOPS; OROBOROS Instruments). Muscle fibers were permeabilized with saponin according to the technique of Veksler et al. (45). After completion of the permeabilization protocol, oxygen consumption was quantified polarographically using a 2-chamber Oxygraph (OROBOROS Instruments) as described earlier (44, 46). Briefly, state 2 respiration was measured after the addition of malate plus glutamate or malate plus octanoyl-carnitine. Subsequently, ADP was added to evaluate state 3 respiration. Coupled respiration was then maximized via addition of succinate. Finally, the chemical uncoupler FCCP was titrated to evaluate the maximal capacity of the electron transport chain (state U) or oligomycin was added to determine respiration not coupled to ATP synthesis (state 4). The integrity of the outer mitochondrial membrane was evaluated by addition of cytochrome *c* upon maximal coupled respiration. All measurements were performed in quadruplets. One muscle biopsy failed before cold acclimation; therefore the values presented are from 16 subjects in total (8 male/8 female).

Mitochondrial isolation. If sufficient biopsy material was obtained, SM mitochondria were isolated as previously described (47) with minor modifications. Briefly, biopsy samples (~200 mg) were placed in ice-cold isolation buffer (100 mmol/l sucrose, 100 mmol/l KCl, 50 mmol/l Tris HCl, 1 mmol/l KH_2PO_4, 0.1 mmol/l EGTA, 0.2% FA-free BSA [wt/vol], pH 7.4) and finely minced with precooled scissors followed by an enzymatic digestion with protease (Subtilisin A; Sigma-Aldrich) on ice. The muscle pieces were then homogenized in a glass potter tube, and the homogenate was transferred to a centrifuge tube and centrifuged at 1000 *g* for 10 minutes at 4°C. The resulting supernatant was filtered through cheesecloth, transferred to a centrifuge tube. and centrifuged at 10000 *g* for 10 minutes at

4°C. The resulting mitochondrial pellet was resuspended in a small (~20 µl) amount of isolation buffer, and protein content was determined by Fluram assay as previously described (48). Subsequently, high-resolution respirometry was performed using 0.1 mg of mitochondria in a medium consisting of 100 mM sucrose, 20 mK K^+-Tes (pH 7.2), 50 mM KCl, 2 mM $MgCl_2$, 1 mM EDTA, 4 mM KH_2PO_4, 3 mM malate. and 0.1% of FA-free BSA.

Three different protocols were performed. In protocol 1, mitochondria in the presence of 5 mM pyruvate as a substrate and oligomycin (1 µg/ml) to block ATP synthesis (state 4 respiration), were automatically titrated with increasing levels of palmitate (dissolved in 50% ethanol) by a titration pump (OROBOROS Instruments) while respiration was monitored. This protocol was performed in duplicate.

The free concentrations of FAs were calculated using the equation described by Richieri et al. (49). Data for FA concentration response curves were analyzed with the 5-parameter logistic curve fit option of the Sigmaplot 8.0 application.

In protocols 2 and 3, mitochondrial respiration was assessed upon carbohydrate-derived (5 mM pyruvate) and FA-derived (50 µM palmitoyl-CoA plus 2 mM carnitine) substrates, respectively. Subsequently, maximal coupled (state 3) respiration was initiated by the addition of 1 mM of ADP. State 4 respiration was measured as the leak respiration following addition of 1 µg/ml oligomycin. Maximal oxygen flux rates (state U) were obtained by titration of the chemical uncoupler FCCP.

From the muscle tissue taken, we managed to isolate mitochondria from 11 subjects (5 male/6 female) for the FA-induced uncoupling (protocol 1), and due to limitations in available mitochondria, we remained with 9 subjects (3 male/6 female) in the remaining 2 protocols.

WAT browning

Abdominal subcutaneous adipose tissue was rinsed from blood, immediately snap frozen, and stored at –80°C for future analyses. Total RNA was isolated from human adipose and muscle biopsies by TRI Reagent (Sigma-Aldrich) extraction and purification using QIAGEN RNeasy Mini Columns according to the manufacturer's instructions. Then 900 ng of total RNA was reverse transcribed and analyzed using Applied Biosystems Real-time PCR Systems using the ΔΔCT method. Relative gene expression was normalized to TATA boxing-binding protein (*tbp*) mRNA levels. Similar results were obtained when relative

expression levels were normalized to 2 additional housekeeping genes: β-2-microglobulin (*B2M*) and cyclophilin A (*PPIA*). Technical replicates were performed, and similar results were observed. Relative gene expression of *UCP1*, *CIDEA*, *PRDM16*, *PGC1a*, *AP2*, *PPAR*γ, adiponectin, adipsin, leptin, *FNDC5*, *TMEM26*, and *CD137* both in WAT and in SM tissue was analyzed (real-time RT-PCR Primer Sequences in Supplemental Table 1 and Supplemental Methods).

Blood analysis

Blood was collected for analyses of several blood parameters. Plasma concentrations of glucose (ABX Glucose HK CP, Radiometer, Horiba ABX), free glycerol (Glycerol kit; R-Biopharm), and total glycerol (ABX Triglycerides CP, Radiometer, Horiba ABX) were determined on a COBAS FARA centrifugal spectrophotometer (Roche Diagnostica). Triglyceride levels were calculated by using the difference in total and free glycerol. Plasma catecholamines were determined using reagents from Recipe (Recipe Chemicals and Instruments) and analyzed on HPLC and by electrochemical detection. Serum insulin was analyzed with a Human Insulin Specific RIA Kit (Millipore) on a Gamma Counter (2470 Automatic Gamma Counter Wizard; Wallac, PerkinElmer). Serum TSH was measured by an Electrochemiluminescence Immunoassay Kit on a COBAS 6000 system (Roche Diagnostica), and free thyroxin (FT4) was analyzed by a solid-phase time-resolved fluoroimmunoassay FT4 kit on an AutoDELFIA system (PerkinElmer). Plasma inflammatory marker C-reactive protein (CRP) was measured with a particle-enhanced immunoturbidimetric assay on a COBAS c311 system (Roche Diagnostics GmbH), and IL-6 and IL-8 were measured with a chemiluminescent immunometric assay on an IMMULITE 1000 system (Siemens).

Statistics

Statistical analyses were performed with PASW Statistics 20.0 for Mac (SPSS). Two-sided paired sample *t* tests were used to compare findings between thermoneutral and mild cold conditions and to test the acclimation effects. Two-sided independent sample *t* tests were used to compare findings between men and women. Spearman rank correlation was used to identify correlations between variables. $P < 0.05$ was considered statistically significant.

Study approval

The ethics committee of Maastricht University Medical Centre+ approved the study protocol, and all subjects provided written informed consent. All procedures were conducted according to the principles of the Declaration of Helsinki.

[–] Supplemental data

View Supplemental data (/articles/view/68993/sd/1)

[–] Acknowledgments

This work is financed by the Netherlands Organization for Scientific Research (TOP 91209037 to W.D. van Marken Lichtenbelt) and by the EU FP7 project DIABAT (HEALTH-F2-2011-278373 to W.D. van Marken Lichtenbelt). We thank Sabina Paglialunga and Kyra Jansen (Maastricht University Medical Centre+) for assistance during the experiments and Ivo Pooters, Matthias Bauwens, Nancy Hendrix, Paul Menheere, and Jos Stegen (Maastricht University Medical Centre+) for their assistance with the biochemical analyses. Furthermore technical support of Boris Kingma, Roel Wierts, Loek Wouters, and Paul Schoffelen (Maastricht University Medical Centre+) is highly appreciated. Finally, we thank our Literature Club for all the fruitful discussions.

[–] Footnotes

Conflict of interest: The authors have declared that no conflict of interest exists.

Citation for this article:*J Clin Invest.* 2013;123(8):3395–3403. doi:10.1172/JCI68993.

[–] References

1. van Marken Lichtenbelt WD, et al. Cold-activated brown adipose tissue in healthy men. *N Engl J Med.* 2009;360(15):1500–1508.
View this article via: PubMed (http://www.ncbi.nlm.nih.gov/pubmed/19357405) CrossRef (http://dx.doi.org/10.1056/NEJMoa0808718)Google Scholar (/references/scholar/31507/B1)

2. Virtanen KA, et al. Functional brown adipose tissue in healthy adults. *N Engl J Med.* 2009;360(15):1518–1525.

View this article via: PubMed (http://www.ncbi.nlm.nih.gov/pubmed/19357407) CrossRef (http://dx.doi.org/10.1056/NEJMoa0808949)Google Scholar (/references/scholar/31507/B2)

3. Muzik O, Mangner TJ, Granneman JG. Assessment of oxidative metabolism in brown fat using PET imaging. *Front Endocrinol (Lausanne).* 2012;3:15.

View this article via: PubMed (http://www.ncbi.nlm.nih.gov/pubmed/22649408)Google Scholar (/references/scholar/31507/B3)

4. Ouellet V, et al. Brown adipose tissue oxidative metabolism contributes to energy expenditure during acute cold exposure in humans. *J Clin Invest.* 2012;122(2):545–552.

View this article via: JCI.org (http://dx.doi.org/10.1172/JCI60433) PubMed (http://www.ncbi.nlm.nih.gov/pubmed/22269323) CrossRef (http://dx.doi.org/10.1172/JCI60433)Google Scholar (/references/scholar/31507/B4)

5. Vijgen GH, Bouvy ND, Teule GJ, Brans B, Schrauwen P, van Marken Lichtenbelt WD. Brown adipose tissue in morbidly obese subjects. *PLoS One.* 2011;6(2):e17247.

View this article via: PubMed (http://www.ncbi.nlm.nih.gov/pubmed/21390318) CrossRef (http://dx.doi.org/10.1371/journal.pone.0017247)Google Scholar (/references/scholar/31507/B5)

6. Saito M, et al. High incidence of metabolically active brown adipose tissue in healthy adult humans: effects of cold exposure and adiposity. *Diabetes.* 2009;58(7):1526–1531.

View this article via: PubMed (http://www.ncbi.nlm.nih.gov/pubmed/19401428) CrossRef (http://dx.doi.org/10.2337/db09-0530)Google Scholar (/references/scholar/31507/B6)

7. Yoneshiro T, et al. Brown adipose tissue, whole-body energy expenditure, and thermogenesis in healthy adult men. *Obesity (Silver Spring).* 2011;19(1):13–16.

View this article via: PubMed (http://www.ncbi.nlm.nih.gov/pubmed/20448535) CrossRef (http://dx.doi.org/10.1038/oby.2010.105)Google Scholar (/references/scholar/31507/B7)

8. Cannon B, Nedergaard J. Metabolic consequences of the presence or absence of the thermogenic capacity of brown adipose tissue in mice (and probably in humans). *Int J Obes (Lond).* 2010;34(suppl 1):S7–S16.

View this article via: PubMed (http://www.ncbi.nlm.nih.gov/pubmed/20935668) CrossRef (http://dx.doi.org/10.1038/ijo.2010.177)Google Scholar (/references/scholar/31507/B8)

9. Nedergaard J, Golozoubova V, Matthias A, Asadi A, Jacobsson A, Cannon B. UCP1: the only protein able to mediate adaptive non-shivering thermogenesis and metabolic inefficiency. *Biochim Biophys Acta.* 2001;1504(1):82–106.

View this article via: PubMed (http://www.ncbi.nlm.nih.gov/pubmed/11239487)Google Scholar (/references/scholar/31507/B9)

10. Cannon B, Nedergaard J. Brown adipose tissue: function and physiological significance. *Physiol Rev.* 2004;84(1):277–359.

View this article via: PubMed (http://www.ncbi.nlm.nih.gov/pubmed/14715917) CrossRef (http://dx.doi.org/10.1152/physrev.00015.2003)Google Scholar (/references/scholar/31507/B10)

11. Davis TR. Chamber cold acclimatization in man. *J Appl Physiol.* 1961;16:1011–1015.

View this article via: PubMed (http://www.ncbi.nlm.nih.gov/pubmed/13883973)Google Scholar (/references/scholar/31507/B11)

12. van Ooijen AM, van Marken Lichtenbelt WD, van Steenhoven AA, Westerterp KR. Seasonal changes in metabolic and temperature responses to cold air in humans. *Physiol Behav.* 2004;82(2–3):545–553.

View this article via: PubMed (http://www.ncbi.nlm.nih.gov/pubmed/15276821) CrossRef (http://dx.doi.org/10.1016/j.physbeh.2004.05.001)Google Scholar (/references/scholar/31507/B12)

13. Cypess AM, et al. Identification and importance of brown adipose tissue in adult humans. *N Engl J Med.* 2009;360(15):1509–1517.

View this article via: PubMed (http://www.ncbi.nlm.nih.gov/pubmed/19357406) CrossRef (http://dx.doi.org/10.1056/NEJMoa0810780)Google Scholar (/references/scholar/31507/B13)

14. Geiser F. Metabolic rate and body temperature reduction during hibernation and daily torpor. *Annu Rev Physiol.* 2004;66:239–274.

View this article via: PubMed (http://www.ncbi.nlm.nih.gov/pubmed/14977403) CrossRef (http://dx.doi.org/10.1146/annurev.physiol.66.032102.115105)Google Scholar (/references/scholar/31507/B14)

15. Wijers SL, Saris WH, van Marken Lichtenbelt WD. Cold-induced adaptive thermogenesis in lean and obese. *Obesity (Silver Spring).* 2010;18(6):1092–1099.

View this article via: PubMed (http://www.ncbi.nlm.nih.gov/pubmed/20360754) CrossRef (http://dx.doi.org/10.1038/oby.2010.74)Google Scholar (/references/scholar/31507/B15)

16. Simonyan RA, Jimenez M, Ceddia RB, Giacobino JP, Muzzin P, Skulachev VP. Cold-

induced changes in the energy coupling and the UCP3 level in rodent skeletal muscles. *Biochim Biophys Acta.* 2001;1505(2–3):271–279.

View this article via: PubMed (http://www.ncbi.nlm.nih.gov/pubmed/11334791)Google Scholar (/references/scholar/31507/B16)

17. Mollica MP, et al. Cold exposure differently influences mitochondrial energy efficiency in rat liver and skeletal muscle. *FEBS Lett.* 2005;579(9):1978–1982.

View this article via: PubMed (http://www.ncbi.nlm.nih.gov/pubmed/15792806) CrossRef (http://dx.doi.org/10.1016/j.febslet.2005.02.044)Google Scholar (/references/scholar/31507/B17)

18. Simonsen L, Bulow J, Madsen J, Christensen NJ. Thermogenic response to epinephrine in the forearm and abdominal subcutaneous adipose tissue. *Am J Physiol.* 1992;263(5 pt 1):E850–E855.

View this article via: PubMed (http://www.ncbi.nlm.nih.gov/pubmed/1443116)Google Scholar (/references/scholar/31507/B18)

19. Wijers SL, Schrauwen P, Saris WH, van Marken Lichtenbelt WD. Human skeletal muscle mitochondrial uncoupling is associated with cold induced adaptive thermogenesis. *PLoS One.* 2008;3(3):e1777.

View this article via: PubMed (http://www.ncbi.nlm.nih.gov/pubmed/18335051) CrossRef (http://dx.doi.org/10.1371/journal.pone.0001777)Google Scholar (/references/scholar/31507/B19)

20. Shabalina IG, Ost M, Petrovic N, Vrbacky M, Nedergaard J, Cannon B. Uncoupling protein-1 is not leaky. *Biochim Biophys Acta.* 2010;1797(6–7):773–784.

View this article via: PubMed (http://www.ncbi.nlm.nih.gov/pubmed/20399195)Google Scholar (/references/scholar/31507/B20)

21. Frontini A, Cinti S. Distribution and development of brown adipocytes in the murine and human adipose organ. *Cell Metab.* 2010;11(4):253–256.

View this article via: PubMed (http://www.ncbi.nlm.nih.gov/pubmed/20374956) CrossRef (http://dx.doi.org/10.1016/j.cmet.2010.03.004)Google Scholar (/references/scholar/31507/B21)

22. Wu J, et al. Beige adipocytes are a distinct type of thermogenic fat cell in mouse and human. *Cell.* 2012;150(2):366–376.

View this article via: PubMed (http://www.ncbi.nlm.nih.gov/pubmed/22796012) CrossRef (http://dx.doi.org/10.1016/j.cell.2012.05.016)Google Scholar (/references/scholar/31507/B22)

23. Walden TB, Hansen IR, Timmons JA, Cannon B, Nedergaard J. Recruited vs.

nonrecruited molecular signatures of brown, “brite,” and white adipose tissues. *Am J Physiol Endocrinol Metab.* 2012;302(1):E19–E31.

View this article via: PubMed (http://www.ncbi.nlm.nih.gov/pubmed/21828341) CrossRef (http://dx.doi.org/10.1152/ajpendo.00249.2011)Google Scholar (/references/scholar/31507/B23)

24. Sharp LZ, et al. Human BAT possesses molecular signatures that resemble beige/brite cells. *PLoS One.* 2012;7(11):e49452.

    View this article via: PubMed (http://www.ncbi.nlm.nih.gov/pubmed/23166672) CrossRef (http://dx.doi.org/10.1371/journal.pone.0049452)Google Scholar (/references/scholar/31507/B24)

25. Gonzalez Rodriguez E, Hernandez A, Dibner C, Koehler Ballan B, Pechere-Bertschi A. [Arterial blood pressure circadian rhythm: significance and clinical implications]. *Rev Med Suisse.* 2012;8(353):1709–1712.

    View this article via: PubMed (http://www.ncbi.nlm.nih.gov/pubmed/23029984)Google Scholar (/references/scholar/31507/B25)

26. Vosselman MJ, et al. Systemic beta-adrenergic stimulation of thermogenesis is not accompanied by brown adipose tissue activity in humans. *Diabetes.* 2012;61(12):3106–3113.

    View this article via: PubMed (http://www.ncbi.nlm.nih.gov/pubmed/22872233) CrossRef (http://dx.doi.org/10.2337/db12-0288)Google Scholar (/references/scholar/31507/B26)

27. Orava J, et al. Different metabolic responses of human brown adipose tissue to activation by cold and insulin. *Cell Metab.* 2011;14(2):272–279.

    View this article via: PubMed (http://www.ncbi.nlm.nih.gov/pubmed/21803297) CrossRef (http://dx.doi.org/10.1016/j.cmet.2011.06.012)Google Scholar (/references/scholar/31507/B27)

28. Kildeso J, Wyon D, Skov T, Schneider T. Visual analogue scales for detecting changes in symptoms of the sick building syndrome in an intervention study. *Scand J Work Environ Health.* 1999;25(4):361–367.

    View this article via: PubMed (http://www.ncbi.nlm.nih.gov/pubmed/10505662) CrossRef (http://dx.doi.org/10.5271/sjweh.446)Google Scholar (/references/scholar/31507/B28)

29. Bartelt A, et al. Brown adipose tissue activity controls triglyceride clearance. *Nat Med.* 2011;17(2):200–205.

    View this article via: PubMed (http://www.ncbi.nlm.nih.gov/pubmed/21258337) CrossRef (http://dx.doi.org/10.1038/nm.2297)Google Scholar (/references/scholar/31507/B29)

30. Cinti S. Reversible physiological transdifferentiation in the adipose organ. *Proc Nutr*

Soc. 2009;68(4):340–349.

View this article via: PubMed (http://www.ncbi.nlm.nih.gov/pubmed/19698198) CrossRef (http://dx.doi.org/10.1017/S0029665109990140)Google Scholar (/references/scholar/31507/B30)

31. Barbatelli G, et al. The emergence of cold-induced brown adipocytes in mouse white fat depots is determined predominantly by white to brown adipocyte transdifferentiation. *Am J Physiol Endocrinol Metab.* 2010;298(6):E1244–E1253.

    View this article via: PubMed (http://www.ncbi.nlm.nih.gov/pubmed/20354155) CrossRef (http://dx.doi.org/10.1152/ajpendo.00600.2009)Google Scholar (/references/scholar/31507/B31)

32. Wijers SL, Saris WH, van Marken Lichtenbelt WD. Individual thermogenic responses to mild cold and overfeeding are closely related. *J Clin Endocrinol Metab.* 2007;92(11):4299–4305.

    View this article via: PubMed (http://www.ncbi.nlm.nih.gov/pubmed/17785356) CrossRef (http://dx.doi.org/10.1210/jc.2007-1065)Google Scholar (/references/scholar/31507/B32)

33. Silva JE. Physiological importance and control of non-shivering facultative thermogenesis. *Front Biosci (Schol Ed).* 2011;3:352–371.

    View this article via: PubMed (http://www.ncbi.nlm.nih.gov/pubmed/21196381) CrossRef (http://dx.doi.org/10.2741/s156)Google Scholar (/references/scholar/31507/B33)

34. Vybíral S, Lesna I, Jansky L, Zeman V. Thermoregulation in winter swimmers and physiological significance of human catecholamine thermogenesis. *Exp Physiol.* 2000;85(3):321–326.

    View this article via: PubMed (http://www.ncbi.nlm.nih.gov/pubmed/10825419) CrossRef (http://dx.doi.org/10.1017/S0958067000019096)Google Scholar (/references/scholar/31507/B34)

35. Wijers SL, Schrauwen P, van Baak MA, Saris WH, van Marken Lichtenbelt WD. Beta-adrenergic receptor blockade does not inhibit cold-induced thermogenesis in humans: possible involvement of brown adipose tissue. *J Clin Endocrinol Metab.* 2011;96(4):E598–E605.

    View this article via: PubMed (http://www.ncbi.nlm.nih.gov/pubmed/21270329) CrossRef (http://dx.doi.org/10.1210/jc.2010-1957)Google Scholar (/references/scholar/31507/B35)

36. Seale P, et al. PRDM16 controls a brown fat/skeletal muscle switch. *Nature.* 2008;454(7207):961–967.

    View this article via: PubMed (http://www.ncbi.nlm.nih.gov/pubmed/18719582) CrossRef (http://dx.doi.org/10.1038/nature07182)Google Scholar (/references/scholar/31507/B36)

37. Schellen L, van Marken Lichtenbelt WD, Loomans MG, Toftum J, de Wit MH. Differences between young adults elderly in thermal comfort, productivity, thermal physiology in response to a moderate temperature drift a steady-state condition. *Indoor Air.* 2010;20(4):273–283.

View this article via: PubMed (http://www.ncbi.nlm.nih.gov/pubmed/20557374) CrossRef (http://dx.doi.org/10.1111/j.1600-0668.2010.00657.x)Google Scholar (/references/scholar/31507/B37)

38. Coyne MD, Kesick CM, Doherty TJ, Kolka MA, Stephenson LA. Circadian rhythm changes in core temperature over the menstrual cycle: method for noninvasive monitoring. *Am J Physiol Regul Integr Comp Physiol.* 2000;279(4):R1316–R1320.

View this article via: PubMed (http://www.ncbi.nlm.nih.gov/pubmed/11003999)Google Scholar (/references/scholar/31507/B38)

39. Charkoudian N, Stephens DP, Pirkle KC, Kosiba WA, Johnson JM. Influence of female reproductive hormones on local thermal control of skin blood flow. *J Appl Physiol.* 1999;87(5):1719–1723.

View this article via: PubMed (http://www.ncbi.nlm.nih.gov/pubmed/10562614)Google Scholar (/references/scholar/31507/B39)

40. Bergstrom J, Hermansen L, Hultman E, Saltin B. Diet, muscle glycogen and physical performance. *Acta Physiol Scand.* 1967;71:140–150.

View this article via: PubMed (http://www.ncbi.nlm.nih.gov/pubmed/5584523) CrossRef (http://dx.doi.org/10.1111/j.1748-1716.1967.tb03720.x)Google Scholar (/references/scholar/31507/B40)

41. van Marken Lichtenbelt WD, et al. Evaluation of wireless determination of skin temperature using iButtons. *Physiol Behav.* 2006;88(4–5):489–497.

View this article via: PubMed (http://www.ncbi.nlm.nih.gov/pubmed/16797616) CrossRef (http://dx.doi.org/10.1016/j.physbeh.2006.04.026)Google Scholar (/references/scholar/31507/B41)

42. Patlak CS, Blasberg RG, Fenstermacher JD. Graphical evaluation of blood-to-brain transfer constants from multiple-time uptake data. *J Cereb Blood Flow Metab.* 1983;3(1):1–7.

View this article via: PubMed (http://www.ncbi.nlm.nih.gov/pubmed/6822610) CrossRef (http://dx.doi.org/10.1038/jcbfm.1983.1)Google Scholar (/references/scholar/31507/B42)

43. Virtanen KA, et al. Human adipose tissue glucose uptake determined using [(18)F]-fluoro-deoxy-glucose ([(18)F]FDG) PET in combination with microdialysis. *Diabetologia.* 2001;44(12):2171–2179.

View this article via: PubMed (http://www.ncbi.nlm.nih.gov/pubmed/11793018) CrossRef (http://dx.doi.org/10.1007/s001250100026)Google Scholar (/references/scholar/31507/B43)

44. Phielix E, et al. Lower intrinsic ADP-stimulated mitochondrial respiration underlies in vivo mitochondrial dysfunction in muscle of male type 2 diabetic patients. *Diabetes.* 2008;57(11):2943–2949.

    View this article via: PubMed (http://www.ncbi.nlm.nih.gov/pubmed/18678616) CrossRef (http://dx.doi.org/10.2337/db08-0391)Google Scholar (/references/scholar/31507/B44)

45. Veksler VI, Kuznetsov AV, Sharov VG, Kapelko VI, Saks VA. Mitochondrial respiratory parameters in cardiac tissue: a novel method of assessment by using saponin-skinned fibers. *Biochim Biophys Acta.* 1987;892(2):191–196.

    View this article via: PubMed (http://www.ncbi.nlm.nih.gov/pubmed/3593705)Google Scholar (/references/scholar/31507/B45)

46. Hoeks J, et al. Prolonged fasting identifies skeletal muscle mitochondrial dysfunction as consequence rather than cause of human insulin resistance. *Diabetes.* 2010;59(9):2117–2125.

    View this article via: PubMed (http://www.ncbi.nlm.nih.gov/pubmed/20573749) CrossRef (http://dx.doi.org/10.2337/db10-0519)Google Scholar (/references/scholar/31507/B46)

47. Tonkonogi M, Sahlin K. Rate of oxidative phosphorylation in isolated mitochondria from human skeletal muscle: effect of training status. *Acta Physiol Scand.* 1997;161(3):345–353.

    View this article via: PubMed (http://www.ncbi.nlm.nih.gov/pubmed/9401587) CrossRef (http://dx.doi.org/10.1046/j.1365-201X.1997.00222.x)Google Scholar (/references/scholar/31507/B47)

48. Hoeks J, et al. Mitochondrial function, content and ROS production in rat skeletal muscle: effect of high-fat feeding. *FEBS Lett.* 2008;582(4):510–516.

    View this article via: PubMed (http://www.ncbi.nlm.nih.gov/pubmed/18230360) CrossRef (http://dx.doi.org/10.1016/j.febslet.2008.01.013)Google Scholar (/references/scholar/31507/B48)

49. Richieri GV, Ogata RT, Kleinfeld AM. The measurement of free fatty acid concentration with the fluorescent probe ADIFAB: a practical guide for the use of the ADIFAB probe. *Mol Cell Biochem.* 1999;192(1–2):87–94.

    View this article via: PubMed (http://www.ncbi.nlm.nih.gov/pubmed/10331662) CrossRef (http://dx.doi.org/10.1023/A:1006878421990)Google Scholar (/references/scholar/31507/B49)